Check for updates

JGR Space Physics

RESEARCH ARTICLE
10.1029/2025JA034830

Plasma Dynamics and Structure of Titan's Induced Magnetosphere From Wave, Magnetic Field, and Plasma Measurements

K. Kim[1,2], R. Modolo[3], N. J. T. Edberg[1], M. Morooka[1], N. Romanelli[4,5], C. Moissard[6], M. K. G. Holmberg[7], C. Bertucci[8], J.-J. Berthelier[3], P. Canu[9], R. Piberne[9], A. J. Coates[10], E. Dubinin[11], L. Regoli[12], W. S. Kurth[13], J.-E. Wahlund[1], J. H. Waite[14], and M. K. Dougherty[15]

[1]Swedish Institute of Space Physics, Uppsala, Sweden, [2]Department of Physics and Astronomy, Uppsala University, Uppsala, Sweden, [3]LATMOS/CNRS, Sorbonne Université, UVSQ—Université Paris-Saclay, Paris, France, [4]Department of Astronomy, University of Maryland, College Park, MD, USA, [5]Planetary Magnetospheres Laboratory, NASA Goddard Space Flight Center, Greenbelt, MD, USA, [6]York Plasma Institute, University of York, York, UK, [7]Dunsink Observatory, Dublin, UK, [8]Institute for Astronomy and Space Physics—IAFE, Ciudad Universiteria, Buenos-Aires, Argentina, [9]LPP-Ecole Polytechnique, Palaiseau, France, [10]Mullard Space Science Laboratory, University College London, Dorking, UK, [11]Max Planck Institute for Solar System Research, Gottingen, Germany, [12]Applied Physics Laboratory, John Hopkins University, Laurel, MD, USA, [13]Department of Physics and Astronomy, University of Iowa, Iowa City, IA, USA, [14]Department of Physics and Astronomy, University of Alabama, Tuscaloosa, AL, USA, [15]Department of Physics, Imperial College of Science, Technology and Medicine, Space and Atmospheric Physics Group, London, UK

Key Points:

- We analyze Titan's induced magnetosphere, making use of Cassini RPWS, CAPS, and MAG measurements from 82 flybys
- We derive the first global electron density map of Titan's near environment and delimit an average induced magnetosphere shape
- We identified pickup ions with energies between 10 eV and 3 keV, increasing along the 0.7 mV m^{-1} convective electric field

Supporting Information:

Supporting Information may be found in the online version of this article.

Correspondence to:

K. Kim,
konstantin.kim@irfu.se

Citation:

Kim, K., Modolo, R., Edberg, N. J. T., Morooka, M., Romanelli, N., Moissard, C., et al. (2026). Plasma dynamics and structure of Titan's induced magnetosphere from wave, magnetic field, and plasma measurements. *Journal of Geophysical Research: Space Physics*, *131*, e2025JA034830. https://doi.org/10.1029/2025JA034830

Received 28 OCT 2025
Accepted 10 APR 2026

Author Contributions:

Conceptualization: K. Kim, R. Modolo, N. J. T. Edberg, M. Morooka, N. Romanelli, C. Moissard, M. K. G. Holmberg, C. Bertucci, J.-J. Berthelier, P. Canu, R. Piberne, A. J. Coates, E. Dubinin, L. Regoli, M. K. Dougherty
Data curation: K. Kim, R. Modolo, N. J. T. Edberg, C. Bertucci, J.-J. Berthelier, P. Canu, R. Piberne, A. J. Coates, J. H. Waite, M. K. Dougherty
Formal analysis: K. Kim, R. Modolo, N. J. T. Edberg, N. Romanelli, C. Moissard, C. Bertucci, E. Dubinin, W. S. Kurth

© 2026. The Author(s).
This is an open access article under the terms of the Creative Commons Attribution License, which permits use, distribution and reproduction in any medium, provided the original work is properly cited.

Abstract In this study, we combine Cassini fields and particle observations to investigate Titan's induced magnetosphere from the TA to T82 flybys, including flybys from the Cassini prime, equinox, and part of the solstice mission, to investigate the average location and the shape of Titan's induced magnetosphere. Although earlier studies have provided valuable information on Titan's induced magnetosphere, they were largely based on separate analyses of fields and particle data. We provide an integrated map of electron density and temperature in Titan's near plasma environment to outline the external boundary of the induced magnetosphere. We identify a dense ionospheric region and an extended plasma wake with electron densities ranging between 10^{-2} and 10^{3} cm^{-3}. In addition, we systematize the spatial distribution of pick-up ions at Titan with respect to the background convective electric field. We indicate that pickup ions are found in the positive hemisphere of the Kronian plasma convective electric field. The mass of the observed pickup corresponds to methane group ions, N_2^+ ions as well as protons and molecular hydrogen ions. The Kronian background electric field progressively accelerates these ions, and we estimate its intensity by reconstructing the radial energy gain of this population in response to the convective electric field. We find the estimated from the pickup ions electric field values within 0.05 mV m^{-1} and 1.92 mV m^{-1} range, which is consistent with an estimate of 0.61 mV m^{-1} deduced from $|-\mathbf{v}_{corot} \times \mathbf{B}|$ computation.

1. Introduction

Titan's interaction with Saturn's magnetospheric plasma has been categorized as atmospheric, like that of Mars and Venus, with the solar wind (Barabash, 2012) since the intrinsic magnetic field of Titan is either weak or haven't been detected (Backes et al., 2005; Wei et al., 2010). Therefore, the ionosphere acts as a conductive obstacle, deflecting the incoming flow and creating a draped magnetic field line region, primarily populated with ionospheric or exospheric plasma, known as the induced magnetosphere (Cravens et al., 2010; Wahlund et al., 2014; Waite et al., 2004). This region is important as most of the energy and momentum is transferred here from the incident plasma flow into Titan's plasma environment (Szegö et al., 2000). From observations, significant differences in the structure of the induced magnetosphere and ionosphere have been detected between the inbound and outbound passes and between flybys with similar trajectories, as was the case for the TA and TB flybys (Wahlund et al., 2005). The cause of such short-period variability can be attributed to Cassini's flyby trajectory, Saturn Local Time (SLT) conditions, or other factors, such as the dayside-nightside ionization balance (Ågren et al., 2009; Vigren et al., 2013, 2015). The solar cycle has an impact on the long-period variability of Titan's ionosphere as discussed by, for example (Edberg et al., 2013; Shebanits et al., 2017). Edberg et al. (2015) showed that the electron density in Titan's ionosphere depends on Saturn local time (at higher altitudes

Funding acquisition: R. Modolo, N. J. T. Edberg, M. K. G. Holmberg, J.-E. Wahlund
Investigation: K. Kim, R. Modolo, N. J. T. Edberg, M. Morooka, N. Romanelli
Methodology: K. Kim, R. Modolo, N. J. T. Edberg, M. Morooka, N. Romanelli, C. Moissard, M. K. G. Holmberg, C. Bertucci, J.-J. Berthelier, P. Canu, R. Piberne, A. J. Coates, E. Dubinin, L. Regoli
Project administration: K. Kim, R. Modolo, N. J. T. Edberg
Resources: K. Kim, R. Modolo, N. J. T. Edberg
Software: K. Kim, R. Modolo, N. J. T. Edberg, M. Morooka
Supervision: N. J. T. Edberg, J.-E. Wahlund
Validation: K. Kim, R. Modolo, N. J. T. Edberg, M. Morooka, N. Romanelli, M. K. G. Holmberg
Visualization: K. Kim, R. Modolo, N. J. T. Edberg
Writing – original draft: K. Kim, R. Modolo, N. J. T. Edberg, M. Morooka, C. Moissard, M. K. G. Holmberg, C. Bertucci, J.-J. Berthelier, L. Regoli
Writing – review & editing: K. Kim, R. Modolo, N. J. T. Edberg, M. Morooka, N. Romanelli, C. Moissard, M. K. G. Holmberg, J.-J. Berthelier, L. Regoli, W. S. Kurth, J.-E. Wahlund, J. H. Waite

1,600–2,400 km) and upstream magnetospheric configuration (at lower altitudes 1,100–1,600 km). Chen and Simon (2020) showed that the induced magnetosphere presents some asymmetry in the Saturn-facing/anti-facing side due to the gyromotion of the pickup ions, emphasizing the limitation of the cylindrical asymmetry. Such asymmetry in the direction of the convective electric field has also been observed for the induced magnetosphere of Mars (e.g., Dubinin et al., 2019; Halekas et al., 2017).

Cassini revealed that Saturn's magnetosphere at Titan's orbit was highly variable, dynamic and complex (Arridge, Achilleos, & Guio, 2011; Arridge, André, Bertucci, et al., 2011; Arridge, André, McAndrews, et al., 2011; Arridge et al., 2008). Several studies focused on the classification of the plasma and the magnetic field properties (Bertucci et al., 2009; Kabanovic et al., 2017; Simon et al., 2013), electron and ion distribution functions (Németh et al., 2011; Regoli et al., 2018; Rymer et al., 2009; H. T. Smith & Rymer, 2014), and plasma density variation (M. Morooka et al., 2009) in the upstream of Titan. It was shown that Titan's relative position to the center of Saturn's magnetodisk strongly affects the upstream environment, thus exposing the moon to either dipole-like fields, high-beta plasma close to SLT 12h and planetward, or radially stretched-out fields and low-beta plasma in the midnight, dawn, and dusk sectors (Bertucci et al., 2009; Simon et al., 2013). The variations of the magnetospheric configuration are commonly observed between the inbound and outbound legs, which occur over periods of a few minutes up to several hours. This affects the draping of the magnetic field lines around Titan, and consequently the induced magnetosphere (Simon et al., 2010).

Another important aspect contributing to the formation of the induced magnetosphere at Titan is the pickup ions. At Titan, pickup ions have been observed by Voyager 1 (Hartle et al., 1982) and Cassini (e.g., Hartle et al., 2006). These ions have masses around 16 amu or more and are created from the ionization of Titan's upper atmosphere (above the exobase) and further embedded in the magnetospheric flow. When picked up by the magnetospheric flow, they are accelerated by the convective electric field $\mathbf{E}_{conv} = -\mathbf{v}_{corot} \times \mathbf{B}$, where $\mathbf{v}_{corot}$ is the corotational bulk velocity of the plasma and $\mathbf{B}$ the local magnetic field, providing an ion escape mechanism responsible for the erosion of Titan's atmosphere. In the magnetospheric flow reference frame, these ions form a ring-beam distribution, unstable to the generation of waves (Cravens, 1997). When pickup ions interact with these waves, two processes occur: pitch-angle and energy diffusion (Cravens, 1997). These processes lead to the mixing of pickup ions with the ambient magnetospheric flow. At the same time, the upstream magnetospheric flow is decelerated due to the transfer of momentum to pickup ions and collisions with the upper atmosphere. Theoretical investigations and global hybrid simulations emphasized the asymmetry between the $+\mathbf{E}$ and $-\mathbf{E}$ hemispheres for pickup ions (e.g., Hartle et al., 2006; Modolo & Chanteur, 2008). Because the gyroradius of heavy pickup ions is larger than Titan, they have also been suggested to cause an asymmetry between Titan's Saturn-facing and anti-Saturn-facing hemispheres on the magnetic pile-up profiles (Chen & Simon, 2020). In addition, due to their large gyroradius compared to the neutral scale height, pickup ions appear as narrow beams in velocity space (Hartle et al., 2006, 2011; Hartle & Sittler, 2007).

Titan shares some interaction characteristics with unmagnetized planets, such as Mars and Venus, where energy and momentum are transferred directly into the atmosphere. However, differences arise due to Titan's unique upstream environment. Unlike the solar wind, corotating magnetospheric flow at Titan's orbit is submagnetosonic and sub-Alfvénic (Arridge, André, Bertucci, et al., 2011). Therefore, a bow shock is not formed, and a boundary layer, such as an induced magnetospheric boundary, is less pronounced. In simulations, for example, from Modolo and Chanteur (2008), the induced magnetosphere (or the magnetic pile-up boundary) is indicated by an increase in magnetic field strength on the ram side and a change in the plasma composition. In contrast, from the observational point of view, a (thermal against magnetic) pressure-balanced transition region is rarely observed since Titan's ionosphere is highly magnetized (Bertucci et al., 2008). We thus identify the induced magnetosphere boundary based on the electron density gradient. A characterization of the electron density extended to Titan's induced magnetosphere will help to outline the average external boundary of the induced magnetosphere. By separating the external boundary of the induced magnetosphere, the plasma dynamics can be assessed separately in the upstream of Titan. Outside the IMB, the plasma motion is governed by $\mathbf{E} \times \mathbf{B}$-drift, whereas within the IMB, the electron pressure and Hall electric fields can play a bigger role.

In this work, we statistically investigate the spatial structure of Titan's plasma environment with a focus on characterizing the pickup ion population and convective electric field in the upstream. We make use of both fields and particle measurements, in particular, the magnetometer (MAG) measurements (M. K. Dougherty et al., 2004), particle data (CAPS) (Young et al., 2004), and Radio and Plasma Wave Science (RPWS) observations (Gurnett

21699402, 2026, 4, Downloaded from https://agupubs.onlinelibrary.wiley.com/doi/10.1029/2025JA034830 by Uppsala Universitet, Wiley Online Library on [08/05/2026]. See the Terms and Conditions (https://onlinelibrary.wiley.com/terms-and-conditions) on Wiley Online Library for rules of use; OA articles are governed by the applicable Creative Commons License

21699402, 2026, 4, Downloaded from https://agupubs.onlinelibrary.wiley.com/doi/10.1029/2025JA034830 by Uppsala Universitet, Wiley Online Library on [08/05/2026]. See the Terms and Conditions (https://onlinelibrary.wiley.com/terms-and-conditions) on Wiley Online Library for rules of use; OA articles are governed by the applicable Creative Commons License

et al., 2004). We show an average map of the electron density and temperature using continuous measurements of both during Cassini Titan flybys from TA to T82. We then focus on the estimation of the convective electric field upstream of Titan's IMB and implications on the spatial distribution of the pickup ions. Our analysis shows the presence of a dense region on the ramside of Titan with steep density gradients, and an extended plasma wake region filled with cold and relatively dense electrons. We use it to delimit the external boundary of Titan's induced magnetosphere. The provided results are important for understanding the electromagnetic environment of Titan's plasma environment and how it is affected by both external and internal factors.

The paper is structured as follows: in Section 2, we introduce the approach to combine both wave (Section 2.1) and particle (Section 2.2) data to build continuous electron density and temperature profiles (Section 3.1) for each flyby from TA to T82. In Section 2.3, we describe the reference frames we use in this paper. The global maps of the electron density and temperature around Titan, assuming cylindrical symmetry are presented in Section 3.2. In Section, departing from the cylindrical symmetry, Section 3.3 the description of the pickup ion population through its energy signature, mass composition (Section 3.4), and its organization with respect to the ambient electric field (Section 3.5) is shown, providing a more complete picture of physics. Finally, in Section 4 we discuss the results, and Section 5 summarizes the conclusions of this work.

2. Measurements and Methodology

2.1. Radio and Plasma Wave Science (RPWS): Density and Temperature of the Cold Electrons

The RPWS instrument can be used to measure the electron number density of the thermal plasma close to Titan. Information derived from the upper-hybrid emission data and the Langmuir probe (LP) sweeps provides two independent density estimates for the cold plasma. In this study, we mainly use the electron number density derived from the wave emissions. The upper hybrid emission line, $f_{UH} = \sqrt{f_{ce}^2 + f_{pe}^2}$, with f_{pe} ($\propto\sqrt{n_e}$) the local plasma frequency and f_{ce} the electron cyclotron frequency, has been detected in the range from 1 to several hundreds of kHz and is the most intense and structured emission at Titan. In Titan's ionosphere, given the relatively weak magnetic field strength ≈5 nT, the electron cyclotron frequency is much smaller than the electron plasma frequency and can be neglected ($f_{ce} \leq 1$ kHz, $f_{ce} \ll f_{pe}$), so the upper-hybrid frequency is approximately equal to the electron plasma frequency and f_{UH} provides a direct visualization of electron density profiles. Most of the Titan flybys exhibit f_{UH} signatures either on the Medium-Frequency Receiver (MFR) or on the High-Frequency Receiver (HFR) and electron densities estimated by this method generally agree with the previously published results (e.g., Edberg et al., 2010). In each flyby, the upper-hybrid emission line was digitized with the ViTos visualization tool, which displays the MFR/HFR spectrum for each acquisition. In each wave spectrum, the ViTos tool proposes the frequency of maximum wave intensity; we have confirmed the selected frequency, or we manually selected a new frequency, as the emission frequency f_{UH} for more than 13,000 spectra. Only data with a clear upper-hybrid emission signature were retained. Two consecutive spectra are separated by about 7 s for the low-rate data. A relatively smooth density profile, similar to the wave and the LP data set, is seen when the spacecraft enters or leaves Titan's induced magnetosphere.

The RPWS LP can also provide the electron density and temperature in Titan's ionosphere. By applying a positive or negative bias voltage on the conducting sphere, the electrons are either repelled or attracted to the probe's surface. This results in current-voltage characteristics, from which the electron density and temperature can be derived. We use the RPWS LP sweeps data for the electron temperature in Titan's ionosphere. A thorough analysis of LP sweeps can be found in for example, Gustafsson and Wahlund (2010), M. W. Morooka et al. (2011), Holmberg et al. (2014), Shebanits et al. (2016), Chatain et al. (2021).

2.2. Cassini Plasma Spectrometer (CAPS): Pick-Up Ions and Hot Electrons

The Cassini Plasma Spectrometer (CAPS) (Young et al., 2004) was designed to measure local properties of electrons and ions, for example, distribution function, and consisted of ion (IMS), electron (ELS), and ion beam spectrometers. The CAPS was mounted on the mechanical actuator, which sweeps ≈2π in azimuthal direction every 3 min and 30 s. The electron spectrometer (ELS) observations of the CAPS are used to compute the electron number density in Saturn's magnetosphere and Titan's environment. The CAPS ELS measured the suprathermal electron distribution in the energy range from 0.6 eV to 28 keV with an energy resolution of 17% and an angular resolution of 20°. Moments, and particularly the density, are determined based on the work of Lewis et al. (2008).

21699402, 2026, 4, Downloaded from https://agupubs.onlinelibrary.wiley.com/doi/10.1029/2025JA034830 by Uppsala Universitet, Wiley Online Library on [08/05/2026]. See the Terms and Conditions (https://onlinelibrary.wiley.com/terms-and-conditions) on Wiley Online Library for rules of use; OA articles are governed by the applicable Creative Commons License

In this study, the CAPS ELS-derived electron moments V1.0 data set is used (Waite, 2022). The CAPS IMS observations have also been used to derive information on the ion population, in particular the mass composition (from the time-of-flight analysis) of plasma for specific time intervals (see Section 3.4) and the pickup ions pitch-angle distribution. The CAPS IMS observes ions in eight angular sectors (similar to ELS) each of them having an identical field of view (FOV) of 8° × 20°. The "singles" (SNG) data product corresponds to energy-per-charge (E/q) spectra ranging from 1 eV to 50 keV with a spectral resolution of 17%. The electrostatic analyzer scanned 8 sweeps, each 4 s long and with 63-step energy steps, referred to as an A-cycle lasting 32 s. The time-of-flight (TOF) analyzer is used to infer detailed compositional analysis for chosen time intervals delivered in so-called B-cycles. During the B-cycle, the 8 angular sectors are summed together, and the 63 energy steps are collapsed to 32 energy steps. In addition, due to telemetry rate limitations, the 2024 mass channels are compressed down to 512 mass channel indices. We have used a B-cycle that lasted 256 s.

Hartle et al. (2006) reported on pickup ion composition for the TA flyby. The TOF analysis suggested the presence of H^+, H_2^+, N^+/CH_2^+, CH_4^+ and N_2^+ with possible contribution of CH_3^+, CH_5^+, $HCNH^+$ and $C_2H_5^+$. When ions enter the CAPS IMS sensor, they first pass through the electrostatic analyzer (ESA) which allow the determination of the energy per charge of the particle. At the exit of the ESA, particles are pre-accelerated and impact a carbon foil, emitting secondary electrons. These electrons are accelerated by the positive ∼15 kV potential and hit the ST detector, giving the start signal of the TOF for the mass identification. When atomic or molecular species pass through the carbon foil, they break down into simpler compounds (neutral particles, positively or negatively charged ions). The neutral atoms and negatively charged particles travel through the TOF chamber and hit the ST detector, producing a stop signal. For a given energy per charge, lighter species will have a shorter time of flight than heavier species and will be identified at smaller TOF channels. The difference of time between the start and the stop signals determines the time of flight. A more detailed description of the CAPS IMS instrument and the mass identification can be found in Young et al. (2004), Hartle et al. (2006), Sittler et al. (2010), Wilson et al. (2012), Thomsen et al. (2014) and in the TOF user guide (H. Smith et al., 2019). The penetrating radiation from the energetic magnetospheric particles from Saturn's radiation belts increases the background count level in all the energy channels. It is caused by the interaction of energetic particles with the microchannel plates of the detector, and can be identified and removed at the postprocessing (e.g., Arridge et al., 2009). This issue is most pronounced in the inner magnetosphere of Saturn and at Titan's orbit it does not play a significant role.

2.3. Reference Frames

There are several reference frames used to present the data in this study. Firstly, the Kronian spherical (KRTP) is used, in which

- $\hat{\mathbf{r}}$ is directed radially away from Saturn,
- $\hat{\theta}$ is directed southward,
- $\hat{\phi}$ is directed parallel to Saturn's equator.

Secondly, the Titan local interaction frame (TIIS) is used, in which

- $\hat{\mathbf{x}}_{TIIS}$-axis is along the ideal corotation direction (or $\hat{\mathbf{x}}_{TIIS} \| \hat{\phi}$),
- $\hat{\mathbf{y}}_{TIIS}$-axis is toward Saturn (or $\hat{\mathbf{y}}_{TIIS} \| - \hat{\mathbf{r}}$),
- $\hat{\mathbf{z}}_{TIIS}$-axis completes the right-handed set (or $\hat{\mathbf{z}}_{TIIS} \| - \hat{\theta}$).

Lastly, the draping system (DRAP) is defined as

- $\hat{\mathbf{x}}_{DRAP}$-axis is aligned with the ideal corotational flow direction,
- $\hat{\mathbf{z}}_{DRAP}$-axis is antiparallel to $B_{z,TIIS}$,
- $\hat{\mathbf{y}}_{DRAP}$ completes the right-handed system.

Such a coordinate system is similar to the DRAP system suggested by Neubauer et al. (2006), except that a non-zero Bx_{DRAP} component is allowed, affecting the location of Titan's neutral sheet. To derive average ambient magnetic fields, it is important to infer time scales for Titan's interaction. In this study, the ambient magnetic field is measured during 20 min, centered at ±1 hr from C/A, for each flyby to ensure that the spacecraft is outside of Titan's induced magnetosphere. The averaged magnetic fields used for this study are different from those

21699402, 2026, 4, Downloaded from https://agupubs.onlinelibrary.wiley.com/doi/10.1029/2025JA034830 by Uppsala Universitet, Wiley Online Library on [08/05/2026]. See the Terms and Conditions (https://onlinelibrary.wiley.com/terms-and-conditions) on Wiley Online Library for rules of use; OA articles are governed by the applicable Creative Commons License

suggested by Simon et al. (2010), who averaged over longer time intervals (about 3 hr inbound and 3 hr outbound). Note that $-\hat{\mathbf{y}}_{DRAP}$ is parallel with the convective electric field.

3. Observations and Analysis

3.1. Combined Measurements From RPWS and CAPS

The CAPS ELS-derived electron density is underestimated in the cold and dense ionosphere of Titan since only part of the electron distribution function is seen due to a negative spacecraft potential and due to a relatively coarse energy resolution compared to the width of the cold electron distribution (Arridge et al., 2009). On the other hand, f_{UH} signatures are not observed below 1–5 kHz (corresponding to an electron number density of 10^{-2} $-3 \cdot 10^{-1}$ cm^{-3}), but are clearly identified for denser ionospheric plasma. While the CAPS ELS is well-designed for hot and tenuous magnetospheric plasma, the RPWS is very well-adapted to measuring cold and dense ionospheric plasma. The complementarity of the two data sets is illustrated in Figure 1. Figure 1 shows electron density in panel (c) and temperature profiles in panel (d) retrieved from different techniques and instruments for the T20 flyby on 25 October 2006.

Several regions with different plasma properties are crossed during the T20 flyby. The spacecraft was first located in Saturn's magnetosphere (before ∼15.45 UTC and after ∼16.10 UTC), characterized by the electron density ranging from 10^{-2}–10^{-1} cm^{-3} and electron temperature of $\approx 10^2$ eV. As Cassini approaches Titan, the electron density progressively increases from 10^{-1} cm^{-3} to $\geq 10^3$ cm^{-3} at the closest approach, while the electron temperature decreases from $\approx 10^2$ eV to 10^{-1} eV. The ionosphere of Titan is characterized by a high electron density, a low electron temperature, and the signature of ionospheric photoelectrons at 10 eV in the CAPS ELS spectra (Coates, 2009). In the ionosphere, the electron densities deduced from the LP data and f_{UH} are almost identical. The closest approach occurred at an altitude of 949 km at 15:51 UTC.

In all analyzed flybys (up to T82), a correspondence between the electron density and temperature estimated from CAPS ELS and RPWS is observed most of the time between 10^{-1} $-$ 1 cm^{-3} density interval, as illustrated in Figure 1. When both CAPS ELS and RPWS measurements were present during the same time interval, RPWS measurements were systematically preferred since they provide direct electron density estimation through the upper-hybrid frequency. The electron temperature profile is a result of combining both LP and CAPS ELS measurements of the electron temperature at a 1 cm^{-3} level. The MAG observations are used to derive information about the background magnetic field environment in the vicinity of Titan, to quantify its variability, and also to emphasize the bipolar tail region reported by Simon et al. (2014). We make use of the Cassini magnetic field high-resolution data in KRTP coordinates (M. Dougherty et al., 2023), transformed into the TIIS coordinate system.

3.2. Electron Density and Temperature Maps

The CAPS ELS- and RPWS-derived electron density estimates are combined to provide a continuous electron density profile extending from Saturn's magnetosphere to Titan's ionosphere for each flyby. All flybys from TA to T82 have been analyzed except T7, T73, T9, and T32, for which no data have been recorded, or a significant deviation from the ideal corotation flow has been observed (e.g., Szego et al., 2007) or the flyby occurred in Saturn's magnetosheath. Figure 2 presents the overall electron density (a) and temperature (c) map of Titan's plasma environment deduced from these combined data sets and corresponding data distribution (b, d). The mean values have been calculated by binning the data on a cylindrical grid (the bin size used is 0.155 R_T or 400 km) where the abscissa is aligned with the $\hat{\mathbf{x}}_{TIIS}$-axis and the ordinate is defined by $\rho_{TIIS} = \sqrt{Y_{TIIS}^2 + Z_{TIIS}^2}$. The cylindrical symmetry with respect to the $\hat{\mathbf{x}}_{TIIS}$-axis is therefore assumed. Similar maps have been presented before in, for example, Edberg et al. (2015), but never with the combined ELS, f_{UH}, and LP data sets. The difference in data distribution of the electron density and temperature is significant in the ionosphere, but has less of an impact in other regions. This is due to the differences in the sampling frequency between the f_{UH}-derived densities, LP-derived density and temperature.

Figure 2a reveals a dense ionospheric region, with values larger than $\geq 10^3$ electrons per cm^{-3}. This result is consistent with previous studies (e.g., Ågren et al., 2009; Edberg et al., 2010). In addition, the density map shows spatial variations in Titan's wake which are attributed to the upstream variability, to a large extent. Note also that

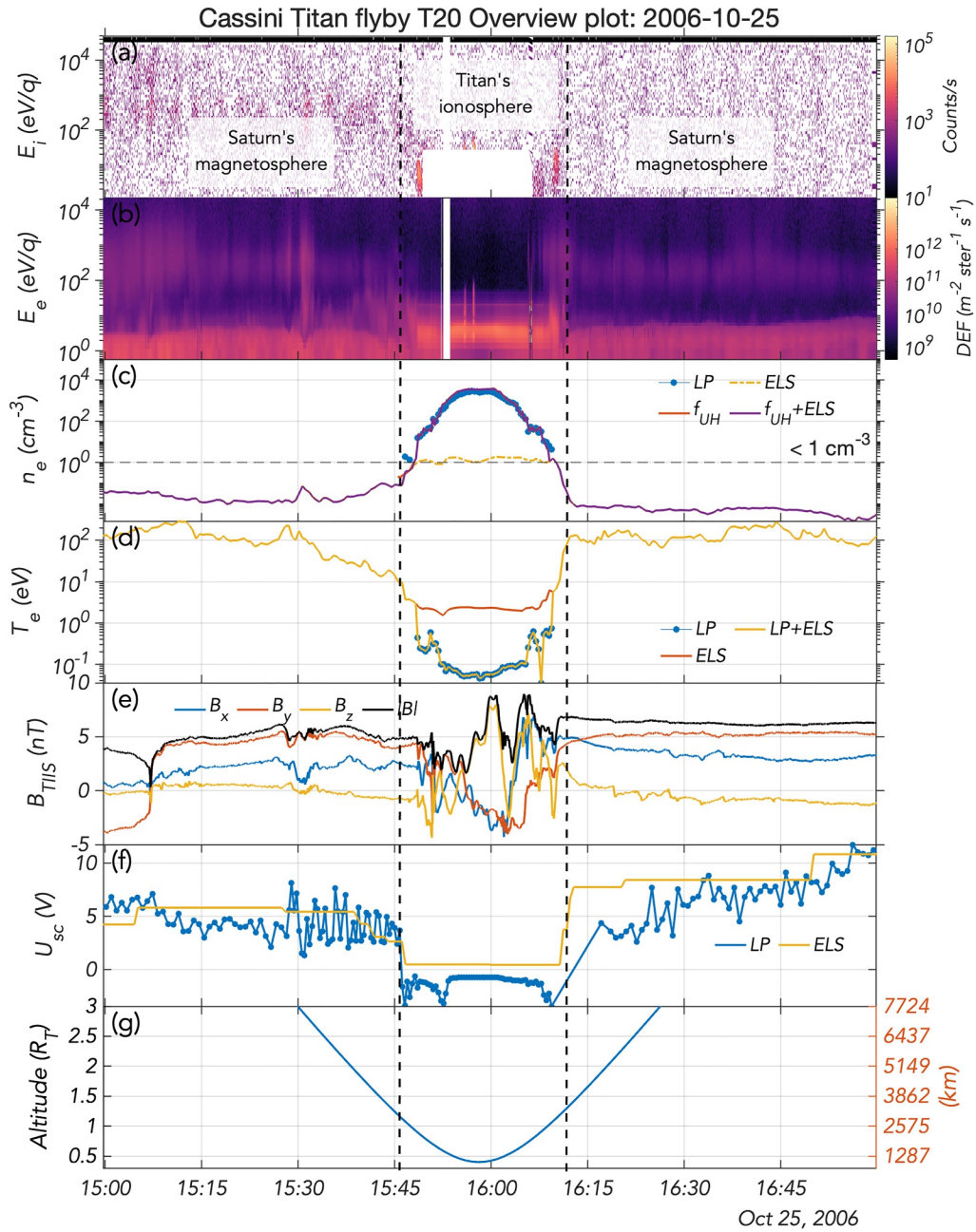

Figure 1. The time series of the plasma and magnetic field measurements: (a, b) ion and electron spectrograms, (c) electron density profiles (blue dots—LP, yellow dashed—ELS, red—f_{UH}, purple—combined f_{UH} and ELS), (d) electron temperature from the LP (blue dots) and ELS (red), and combined (yellow), (e) the three components of the magnetic field in the Titan-interaction coordinate system (TIIS), (f) the spacecraft potential estimated from the LP (blue) and ELS (yellow), (g) altitude profile (R_T = 2575 km). The vertical dashed lines approximately separate Saturn's magnetosphere and Titan's ionosphere.

in some areas, there is poor coverage, and the cylindrical asymmetry might not always be valid. As seen in Figure 1, around 15.50 UTC in the inbound and around 16.15 UTC in the outbound, a sharp electron density gradient is usually observed at the induced magnetosphere boundary. The induced magnetosphere can be roughly identified at locations where the electron number density is between 1 and 10 cm^{-3} since Saturn's magnetospheric plasma does not reach such a density value at Titan's orbit (Wilson, 2021). A similar location of Titan's induced magnetospheric boundary can be derived from the gradient of the density profiles in Figure 2. A more accurate location of the induced magnetosphere may require including criteria based on magnetic field and plasma flow

21699402, 2026, 4, Downloaded from https://agupubs.onlinelibrary.wiley.com/doi/10.1029/2025JA034830 by Uppsala Universitet, Wiley Online Library on [08/05/2026]. See the Terms and Conditions (https://onlinelibrary.wiley.com/terms-and-conditions) on Wiley Online Library for rules of use; OA articles are governed by the applicable Creative Commons License

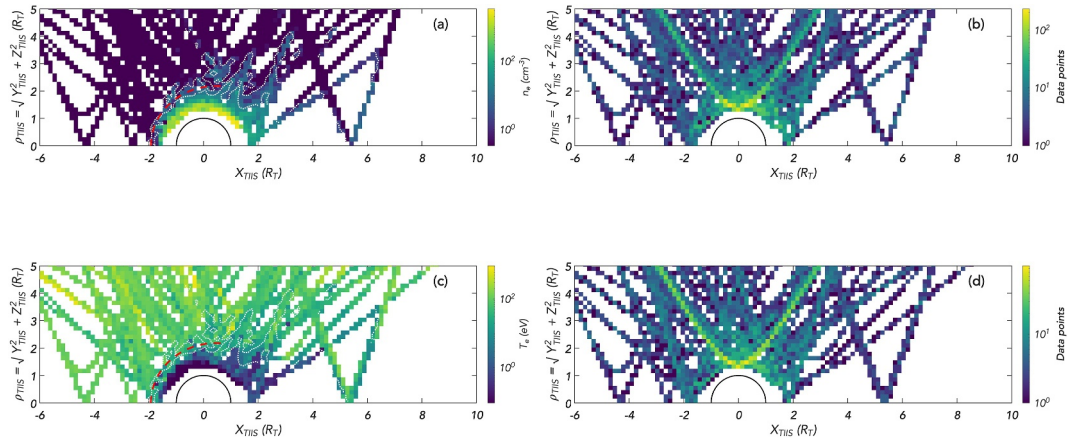

Figure 2. The electron density and temperature maps in a cylindrical Titan-centered frame covering flybys from the TA to T82: (a) electron density and (c) electron temperature maps, (b, d) data points density. The white dashed line corresponds to an isocontour at 1–10 cm^{-3} density that marks the transition region from Saturn's magnetosphere to Titan's ionosphere and is attributed to the induced magnetosphere boundary. The red dashed line is a conic fit $r = \frac{L}{1+\epsilon \cos\theta}$ with parameters $X_0 = -0.5$ R_T, $L = 2$ R_T, $\epsilon = 0.4$.

observations. The electron temperature map in Figure 2c shows several distinct regions. The cold ionosphere has an average electron temperature of $\approx 10^{-1}-10^{0}$ eV, the hot magnetosphere of Saturn with an electron temperature $\geq 10^{1}$ eV, and an extended in $\hat{\mathbf{x}}_{TIIS}$-axis tail of cold electrons in the x-direction, with the same temperature as in the ionosphere. We observe a good statistical sampling of the ionospheric region. Globally, a reasonable sampling was achieved for the induced magnetosphere with more than five samples (from several flybys) in each bin with no statistical bias in the electron density and temperature maps (see Figures 2b and 2d).

To delimit the external boundary of the induced magnetosphere, we have indicated the approximate boundary location in the ram side and the near wake region, up to $X_{TIIS} = 1$ R_T, the $1-10$ cm^{-3} (where the steepest electron density gradient is located) isocontour with a function corresponding to an ellipse. Expressed in polar coordinates, assuming a symmetry along the X_{TIIS} axis, the equation of the induced magnetosphere surface is $r = \frac{L}{1+\epsilon \cos\theta}$ where the polar coordinates (r,θ) are measured about the focus X_0, L is the semi-latus rectum and ϵ is the eccentricity. The fitted conic parameters are $X_0 = -0.5$ R_T, $L = 2$ R_T and $\epsilon = 0.4$. We did not extend the fit in the middle and far Titan's wake beyond $X_{TIIS} = -0.1$ R_T because of the limited coverage. The fit of the induced magnetosphere boundary is represented by the red dashed curve in Figure 2 (both electron and temperature maps). A conic function has also been used to delimit the induced magnetosphere or magnetic pile-up boundary for Mars and Venus (e.g., Bertucci et al., 2011). Although Figure 2 does not show plasma composition, it suggests that plasma of Titan's origin can reach several tens of cm^{-3} at about 3 R_T and several cm^{-3} at about 6 R_T in the tail region. The induced magnetospheric boundary is closer to the planet on the ram side than on the flank side and the plasma scale height is much larger in the wake than on the ram side. From the induced magnetosphere boundary fit, two parameters were determined: $R_{SD} = 1.88$ R_T which is the ellipse stand-off distance along the $\hat{\mathbf{x}}_{TIIS}$-axis and $R_{TD} = 2.15$ R_T which is the ellipse stand-off distance along the ρ_{TIIS}-axis.

3.3. Observations of Pickup Ions

Ions from Titan's exosphere, found in the upstream of the induced magnetosphere and incorporated into the background plasma flow, are so-called pickup ions. Using CAPS IMS observations of ions, we identify and infer the spatial distribution of the pickup ion population in Titan's plasma environment. Regoli et al. (2016) have performed a survey of the pickup ions and found their presence to be mainly on the anti-Saturn side, which leads to the conclusion that CAPS IMS has captured freshly produced pickup ions. In this paper, we go one step further by organizing the pickup ion observations in a reference frame depending on the magnetic field and characterizing their progressive acceleration.

The pickup ions signatures were searched manually in the CAPS IMS data in the TA-T82 flybys. In Figure 3, we show four examples of such signatures found at the edge of Titan's induced magnetosphere, from the TA, T6, T39,

21699402, 2026, 4, Downloaded from https://agupubs.onlinelibrary.wiley.com/doi/10.1029/2025JA034830 by Uppsala Universitet, Wiley Online Library on [08/05/2026]. See the Terms and Conditions (https://onlinelibrary.wiley.com/terms-and-conditions) on Wiley Online Library for rules of use; OA articles are governed by the applicable Creative Commons License

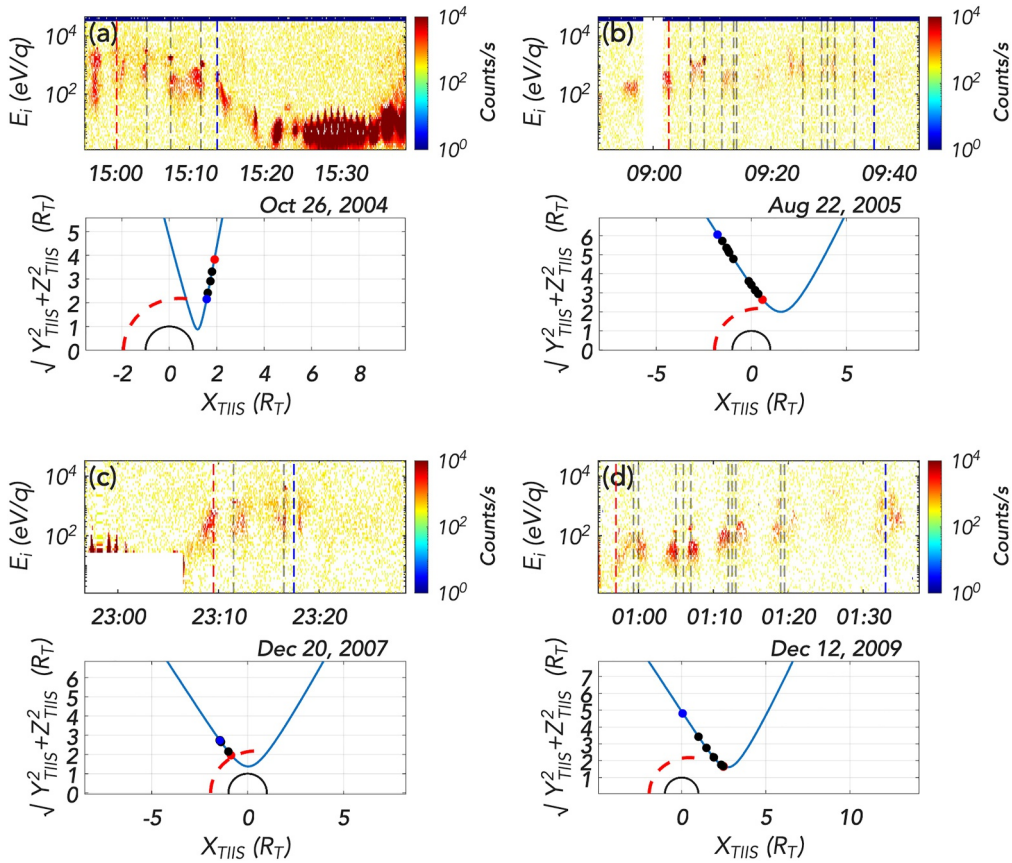

Figure 3. An example of CAPS IMS pickup ions observations during the TA, T6, T39, and T63 flybys. Each set has a top subpanel (a–d) presenting summed over all anodes CAPS IMS observations and a bottom subpanel illustrating the Cassini trajectory (blue line) for the corresponding flyby in the cylindrical TIIS coordinate system. The black dashed lines in the CAPS IMS panels indicate the presence of pickup ions, where red and blue colors show the beginning and the end of the time interval. Their locations are indicated on Cassini's trajectory with circle marks of corresponding red and blue colors. The energy table change on CAPS IMS during the closest approach produces the data gaps at lower energies displayed on panels (b) and (c). The background is saturated to enhance the pickup ion signature.

and T63 flybys. Additional flybys exhibiting similar signatures are shown in Table S1 (see Supporting Information S1). Figure 3 displays the energy spectrogram of the detected pickup ions and their location in cylindrical coordinates. The bottom panels of each set show Cassini trajectories drawn in cylindrical TIIS coordinates, while the top panel displays the summed over all anodes counts measured by CAPS IMS (SNG data set). The patchy and repetitive structures observed in the magnetospheric region are due to the actuator motion of the platform hosting the particle instruments. The colors are artificially saturated to highlight the pickup ion's signature.

For example, in panel (a), we see the progressive deceleration of the incoming plasma on the inbound and outbound legs of each of these flybys and the entry of Cassini into Titan's ionosphere as indicated by low-energy signatures (<10^2 eV) and high particle counts (>10^3 counts s^{-1}). The narrow beam energy signatures, indicated by the black dashed lines, suggest that these features arise from injecting freshly ionized pickup ions, in contrast with pickup ions after several gyrations, which undergo pitch-angle scattering. For these specific observations, the angle between the background magnetic field and the bulk plasma flow (Waite & Furman, 2022) ranges between 70° and 140°. The observed ion pickup energy is smaller than the theoretically expected maximum, given by $4\frac{m_{pi}}{m_{am}}E_{am}\sin^2\theta_{vB}$ where m_{pi}/m_{am} is the ratio between ion pickup mass and the ambient ion mass, E_{am} is the average kinetic energy of the ambient plasma, and θ_{vB} is the angle between the ambient plasma flow velocity and the background magnetic field direction. The location of the observed events is indicated on the Cassini trajectory with black dots. These events occur in the external part of the induced magnetosphere, usually near one of its flank, or in the Kronian plasma region. This finding is consistent with global simulation results which reported

21699402, 2026, 4, Downloaded from https://agupubs.onlinelibrary.wiley.com/doi/10.1029/2025JA034830 by Uppsala Universitet, Wiley Online Library on [08/05/2026]. See the Terms and Conditions (https://onlinelibrary.wiley.com/terms-and-conditions) on Wiley Online Library for rules of use; OA articles are governed by the applicable Creative Commons License

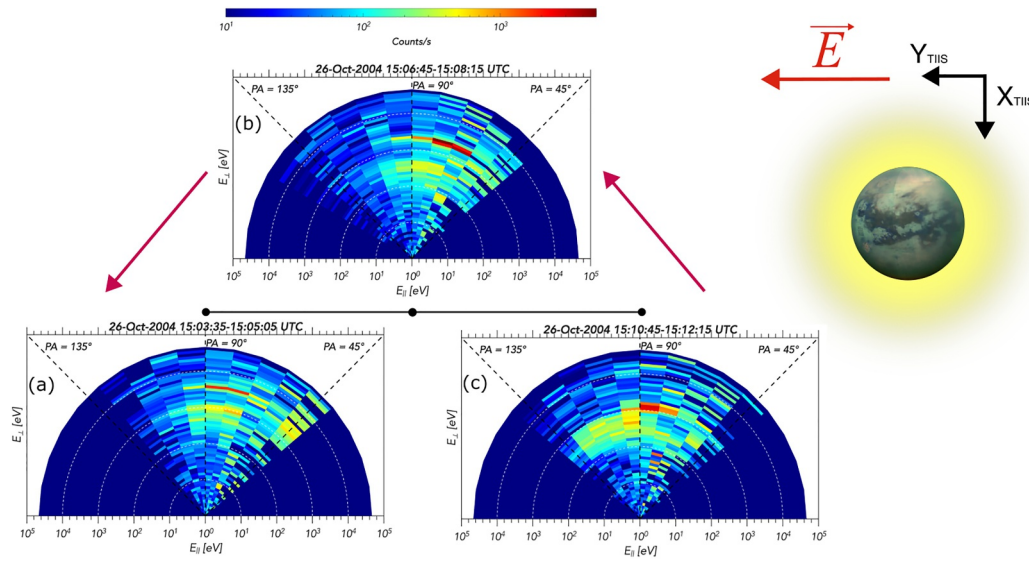

Figure 4. A not-to-scale sketch of the pickup ion pitch-angle distribution radial evolution during the TA flyby. The letters represent different radial distances: (a) 1.76 R_T (4,529 km), (b) 1.39 R_T (3,581 km) and (c) 0.91 R_T (2,352 km). The colorbar is common for all plots and represents the ion counts per second. The red arrow shows the direction of the convective electric field in the upstream of Titan. Black dashed lines indicate three pitch-angles (PA) 45°, 90°, 135°. Red arrows show the radial evolution direction of the ion pitch-angle distribution.

pickup ions with relatively high energy in the flank of the induced magnetosphere, and more precisely in the +**E**-hemisphere according to simulation results and theoretical expectations (e.g., Modolo & Chanteur, 2008, their Figure 7).

In Figure 4, an example of a pickup ion pitch-angle distribution at different radial distances from Titan is shown from the TA flyby in polar (r,θ) coordinates. To compute the pitch-angle, the magnetic field measurements have been averaged during the shown time intervals (see top of sub-figures), which is smaller than, or in the same order as, the heavy pickup ions (~180 s for CH_4^+ ions, ~300 s for N_2^+ ions, Cowee et al. (2010)). Then we calculate the pitch-angle between each angular bin of the IMS FOV and the averaged magnetic field for each energy channel. The r coordinate represents the energy on a logarithmic scale, from 1 eV to 46 keV, while the θ coordinate indicates the pitch angle. The $\pm x$ direction of the plot implies a parallel/anti-parallel direction (with respect to the local magnetic field), and the y direction means a direction perpendicular to the magnetic field. The bulk plasma flow velocity around Titan, $v_b \approx 120$ km s^{-1} (Arridge, André, Bertucci, et al., 2011), is larger than the average spacecraft velocity, $v_{sc} \approx 6$ km s^{-1}). We therefore neglect the impact of $|v_b - v_{sc}|$ difference when calculating the pitch-angle distribution (the limitations of that are discussed in Section 4). As the pickup ions start to undergo **E** × **B**-drift, they experience acceleration by the electric field at different parts of the trajectory. It can be seen that the difference between the PADs at different radial distances from Titan is insignificant. The absence of pitch-angle and energy diffusion can show that wave-particle interactions play a minor role in the ion distribution function evolution up to a certain distance from Titan. However, what we can observe is the increase in energy of the pickup ion population: from nearly 90° with ≈1 keV energy (number 1), to similar pitch-angle and >1 keV energy (number 2), and finally, same pitch-angle and ≈8 keV energy (number 3). As a next step, we analyze each flyby for the presence of narrow injections of ions and check if they are consistent with either one of the discussed parts of the pickup ion's trajectory.

3.4. Pickup Ion Mass Composition

Figure 5 displays the counts of the straight-through (ST) detector as a function of energy per charge versus time of flight. The ion mass composition during the T6 flyby (TOF acquisition from 09.04.45 to 09:13:17 UTC) indicates the presence of pickup ions in a narrow band of energies. The ion energies range from about 10 eV to a few keV, where a mixture of ambient plasma and pickup ions is observed. Thomsen et al. (2010), and Wilson et al. (2017) have presented ion moments at Titan's orbit indicating that H^+, W^+ (water group ions) and H_2^+ are the major

21699402, 2026, 4, Downloaded from https://agupubs.onlinelibrary.wiley.com/doi/10.1029/2025JA034830 by Uppsala Universitet, Wiley Online Library on [08/05/2026]. See the Terms and Conditions (https://onlinelibrary.wiley.com/terms-and-conditions) on Wiley Online Library for rules of use; OA articles are governed by the applicable Creative Commons License

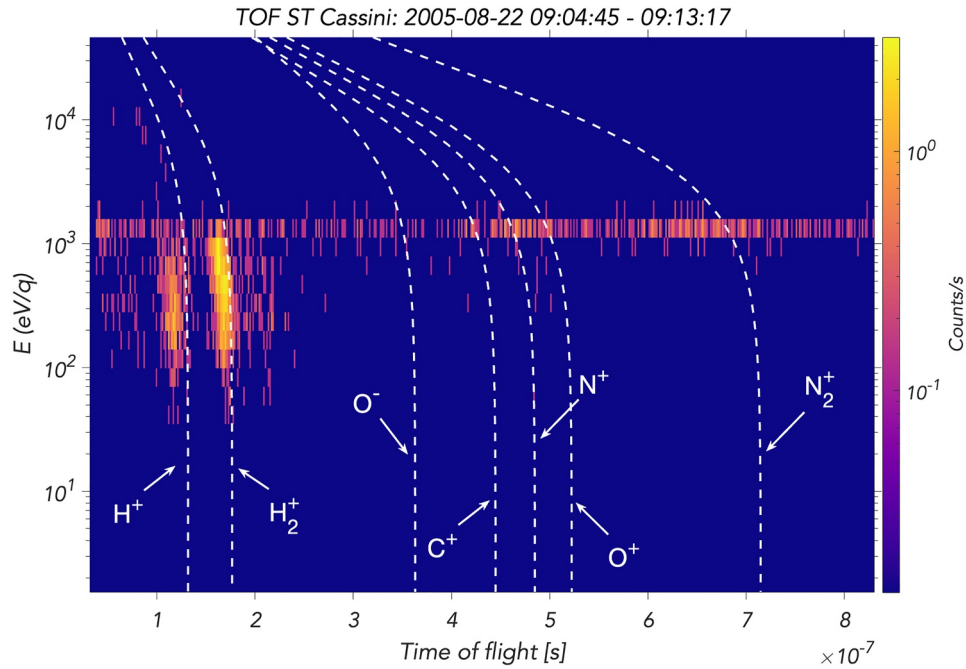

Figure 5. An example of the time-of-flight straight through (TOF ST) spectrum observed during the T6 flyby. The spectrum was obtained by summing over the time interval between 09:04:45 UTC and 09:13:17 UTC. The white dashed lines indicate the theoretical TOF for specific ion species such as H^+, He^{2+}/H_2^+, O^-, C^+, N^+, O^+ and N_2^+—group ions. The extended signal around 1 keV is a typical signature of the pickup ions with m/q > 2.

constituents of the magnetospheric plasma. On the other hand, Felici et al. (2018) have suggested that Titan could also be a source of H_2^+ ions due to a maximum ratio of H_2^+/H^+ near Titan's orbit, assuming that Titan is not in Saturn's magnetosheath or solar wind. This is the case for the T6 flyby and we can attribute the m/q = 2 signatures to H_2^+ ions and not He^{2+} ions. For ions below 1 keV, the compositional analysis reveals H^+ and H_2^+ ions. The ambient plasma differs from the pickup ion population not only in their energy signature but also from their incoming flow direction. The low-energy species represent a different angular distribution compared to the 1 keV species, indicating different flow directions and, therefore, suggesting distinct populations.

At about 1 keV, the TOF ST in Figure 5 spectrogram indicates heavier species. These ion species with an energy slightly above 1 keV correspond to the IMS energy pickup ion identification presented in Figure 3b. In Figure 5, the white dashed lines correspond to the expected signatures when the ST detection is associated with a particle that exits the carbon foil as a neutral. When the charge state is negative, the time of flight will be shorter, but those theoretical curves are not shown. This diagnostic provides a rough estimate of the ion mass composition. The composition is also supported by a simulation model, developed by Nelson and Berthelier (2009), characterizing the IMS instrumental response to various ion compositions at different energies. Simulation results have been compared to the test chamber calibration measurements for several ion masses (atomic and molecular species with masses ranging from 12 to 28 amu) and at different energies (from 1,024 to 27,560 eV). The overall signatures thus indicate that the ion population near the flank of the induced magnetosphere have a m/q of 1, ∼15 and ∼28. With the knowledge of the Titan ionosphere composition, there is a good probability that it corresponds to H^+, CH_3^+ or N_2^+. Thus, this pickup composition for flyby T6 is similar to the TA observations (Hartle et al., 2006). Unfortunately the TOF measurements by CAPS IMS do not always allow determining the mass composition due to an insufficient number of counts on the ST detectors. Nevertheless, when available, they suggest the presence of the methane group (CH_2^+, CH_3^+, CH_4^+, CH_5^+) as well as of heavier species such as H_2CN^+ or N_2^+ (depending on the altitude and the relative abundance of species). The column 7 of Table S1 summarizes the information on the mass composition of pickup ions when mass identification was possible.

21699402, 2026, 4, Downloaded from https://agupubs.onlinelibrary.wiley.com/doi/10.1029/2025JA034830 by Uppsala Universitet, Wiley Online Library on [08/05/2026]. See the Terms and Conditions (https://onlinelibrary.wiley.com/terms-and-conditions) on Wiley Online Library for rules of use; OA articles are governed by the applicable Creative Commons License

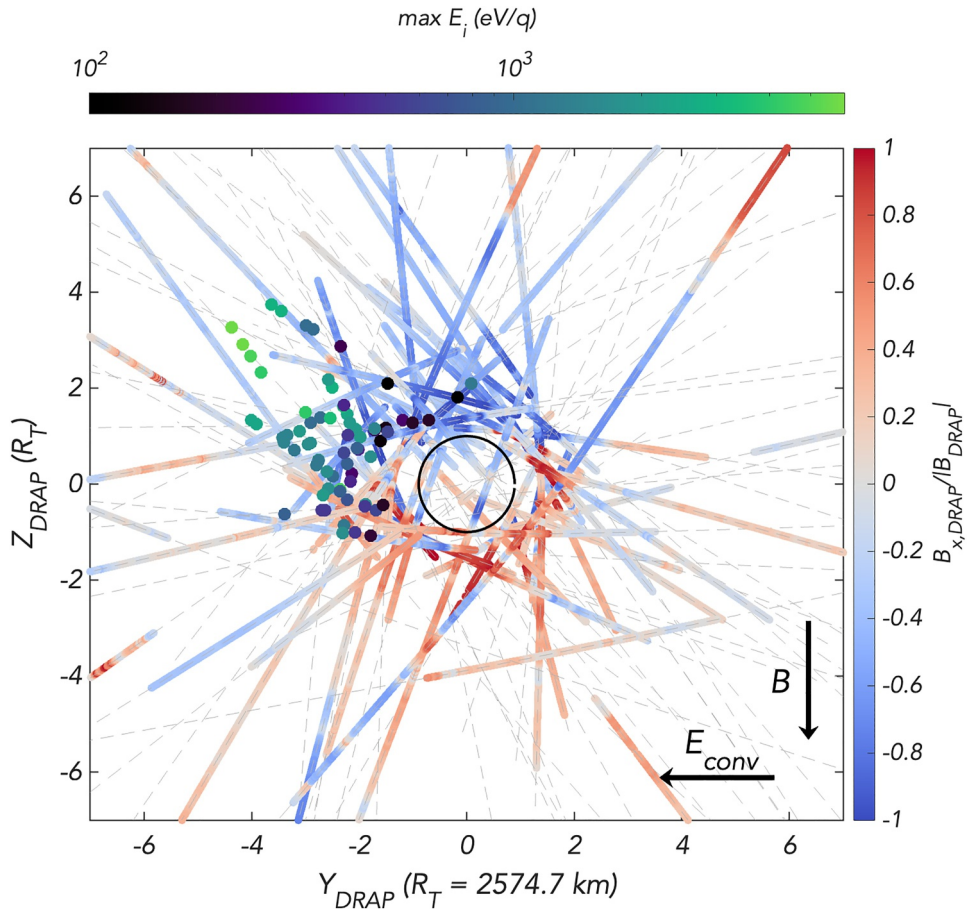

Figure 6. Projection of the Cassini flyby in the YZ_{DRAP} plane. Cassini's trajectories, in the DRAP coordinates, are shown by the dashed lines. Along the trajectory, the $B_{x,DRAP}/|B_{DRAP}|$ are colored, in a blue-red colorbar, only in the induced magnetosphere region, and it emphasizes the two magnetic lobe polarities due to the draping. The horizontal colorbar on top of the figure shows the maximum energy of the observed pickup ions and mark spatial distribution of the pickup ions around Titan.

3.5. Spatial Distribution and Energization of Pickup Ions

The spatial distribution of pickup ions is closely related to the convective electric field and magnetic field orientations outside the induced magnetosphere. We use a draping coordinate system (DRAP) based on the magnetic field direction upstream of the induced magnetosphere to highlight the draped nature of the magnetic field and the relation between the convective electric field and pickup ions. Figure 6 shows a global overview of Titan's induced magnetosphere and the spatial distribution of the pickup ions. It represents the projection of Cassini trajectories in dashed lines in the *YZ* plane of the DRAP coordinate system, depending on the possibility of determining the average upstream magnetic field.

The bipolarity of Titan's induced magnetosphere is emphasized with a clear reversal of the B_x component of the magnetic field, indicating two magnetic lobe structures formed during the interaction of Titan's ionosphere and the Kronian plasma. The local B_x component is plotted along the DRAP trajectory in the region limited in $\hat{\mathbf{x}}$ direction, and the colorscale is shown on the right side. This result is consistent with the magnetotail structure characterized by for example, Simon et al. (2010); Kim et al. (2024). The colorscale (top bar) shows the corresponding energy of the pickup ion signature. From the spatial distribution, it can be seen that pickup ions are observed predominantly in the +**E**-hemisphere. The pickup ions with the lowest energy are observed preferentially in a range of $\hat{\mathbf{z}}_{DRAP}$ values between $\pm$ 2 R_T. A progressive energization is demonstrated since the pickup ions observed farther from Titan reach higher energies up to several keV, comparable to the ambient magnetospheric ions' energy. The gyroradius of pickup ions for m/q = 16 and 28 in a typical Kronian plasma at Titan's orbit is ≈2

21699402, 2026, 4, Downloaded from https://agupubs.onlinelibrary.wiley.com/doi/10.1029/2025JA034830 by Uppsala Universitet, Wiley Online Library on [08/05/2026]. See the Terms and Conditions (https://onlinelibrary.wiley.com/terms-and-conditions) on Wiley Online Library for rules of use; OA articles are governed by the applicable Creative Commons License

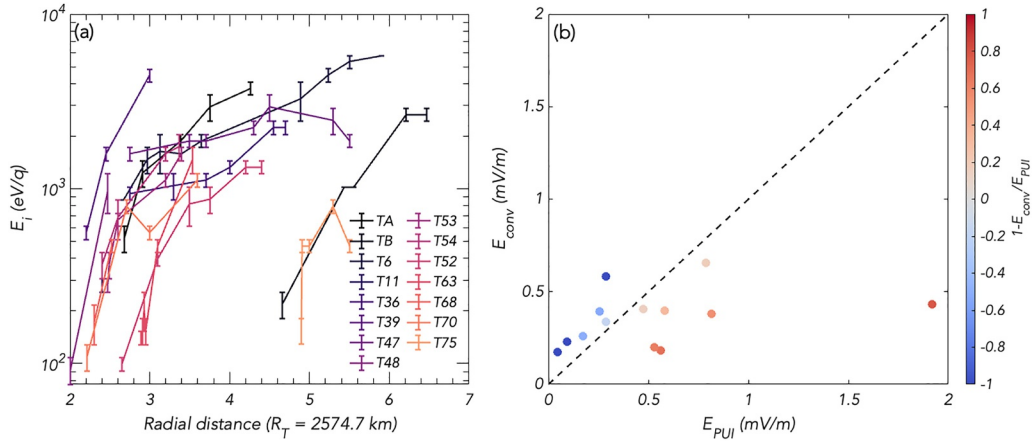

Figure 7. (a) Pickup ion energy (in eV) as a function of radial distance to Titan (in R_T) for different flybys where pickup ions have been identified. The error bars show the energy range of the observed pickup ions (the spread is due to the energy bin resolution). (b) Comparison between the derived from pickup ions $|E_{PUI}|$ and plasma moments $|E_{conv}|$ electric fields. The dashed line indicates the exact correspondence, that is, $|E_{PUI}| = |E_{conv}|$, and the colorcode shows the deviation from the exact match. The presence of fewer data points is due to the absence of ion velocity measurements upstream of Titan.

R_T and ≈3.5 R_T, respectively. Comparing the typical ion gyroradius with the observed pickup distribution in Figure 6, we conclude that CAPS IMS observed the pickup ions in the injection step or during the gyration phase.

Figure 7a shows the energy of the pickup ions as a function of the distance for the flybys with the pickup ion signatures. A linear relationship between the distance to the moon and the energy (up to 5.5 keV) is observed for a majority of flybys. Assuming that the electric field is constant during a flyby outside of the induced magnetosphere, and integrating the equation of motion of a charged particle in a uniform electric field we can show that the energy $\mathcal{E}$ gained by the particle depends on the electric field and the distance of acceleration ($\mathcal{E} = qE_{\perp}x$, with x the distance). A linear regression analysis for each flyby therefore provides an estimate of the intensity of the perpendicular component of the Kronian electric field. We found that the Kronian electric field, estimated from the above-mentioned expression, varies between 0.05 mV m^{-1} and 1.92 mV m^{-1}, depending on flyby.

We then compare the estimated convective electric field $\mathbf{E}_{PUI}$ from the pickup ions with the convective electric field $\mathbf{E}_{conv} = -\mathbf{v}_{corot} \times \mathbf{B}$, calculated from the ion moments and magnetic field. If the ion moments are absent, the comparison is not performed. Figure 7b shows the result of the comparison, and the colorcode shows how much the estimates differ from each other, and the error bars show the min-max range of the observed pickup ion energies. For lower values of the electric field (below 1 mV m^{-1}), the two methods are relatively consistent with each other. At higher values (above 1 mV m^{-1}), there is an outlier at $E_{PUI} \approx 2$ mV m^{-1}, which can be explained by high variability in the upstream magnetic field or corotation flow velocity. With a typical velocity of 140 km s^{-1} along the corotation direction and an average magnetic field of 4.4 nT aligned with the Z_{TIIS} axis, the electric field is $|\mathbf{E}_{conv}| = |-\mathbf{v}_{corot} \times \mathbf{B}| \approx 0.61$ mV m^{-1}, which is in the range of the electric field intensity derived from pickup ions.

4. Discussion

In this study, we focused on the dynamic processes in Titan's induced magnetosphere. We used data from the RPWS, MAG, and CAPS instruments to quantify the electrodynamic and plasma parameters of the environment around Titan during the TA to T82 flybys. The derived electron density and temperature maps provide the average location of an induced magnetosphere boundary, which can be useful in simulations. The results are to be seen as average. Therefore, transient and local effects, such as relative distance to the center of Saturn's magnetospheric current sheet, Saturn Local time variability, are not taken into account. The variability of an ambient environment and how it affects Titan's plasma environment have been emphasized by for example, Bertucci et al. (2009), Garnier et al. (2010), Rymer et al. (2009), Simon et al. (2010), Németh et al. (2011), Edberg et al. (2013), Regoli et al. (2018). The variations in the upstream parameters affect Titan's induced magnetosphere and contribute to blurring the electron density and temperature map. The simulation results are also consistent with this global

21699402, 2026, 4, Downloaded from https://agupubs.onlinelibrary.wiley.com/doi/10.1029/2025JA034830 by Uppsala Universitet, Wiley Online Library on [08/05/2026]. See the Terms and Conditions (https://onlinelibrary.wiley.com/terms-and-conditions) on Wiley Online Library for rules of use; OA articles are governed by the applicable Creative Commons License

21699402, 2026, 4, Downloaded from https://agupubs.onlinelibrary.wiley.com/doi/10.1029/2025JA034830 by Uppsala Universitet, Wiley Online Library on [08/05/2026]. See the Terms and Conditions (https://onlinelibrary.wiley.com/terms-and-conditions) on Wiley Online Library for rules of use; OA articles are governed by the applicable Creative Commons License

electron density map (e.g., Ledvina et al., 2012; Ma et al., 2006; Modolo & Chanteur, 2008; Sillanpää et al., 2006; Simon et al., 2007; Snowden et al., 2007). The lack of coverage in the center of the far tail ($R > 3R_T$ and $\rho < 1R_T$) and the use of a cylindrical representation does not allow a clear distinction of the two ionospheric separated tail structures identified in a few flybys (Coates et al., 2012).

The electron density and temperature map provide an upper limit of the cross-section tail area at different distances in the tail, assuming a cylindrical symmetry, which might be useful to compute the ionospheric loss rate. For instance, Coates et al. (2012) assumed an area of πR_T^2 to compute the escape rate, similar to Modolo, Wahlund, et al. (2007) and Modolo, Chanteur, et al. (2007). According to Figure 2b, the area of this disk might have been underestimated. The effective tail's cross-sectional radius is increased by a factor of 2 (as an upper limit), and therefore, the escape rate is increased by the same factor squared (since the area is $\sim R_T^2$), or a factor of 4. For more detailed analysis, the reader is referred to Wahlund et al. (2005), Coates et al. (2007, 2012), Szego et al. (2007), Modolo, Wahlund, et al. (2007), Modolo, Chanteur, et al. (2007), Sittler et al. (2010), Edberg et al. (2011), Westlake et al. (2012) and Romanelli et al. (2014).

It can be seen that pickup ions are observed predominantly in the +**E**-hemisphere. This is supported by the test-particle and global simulations (e.g., Luhmann, 1996; Modolo & Chanteur, 2008). These pickup ions contribute to the local processes at Titan by decelerating the ambient magnetospheric flow. However, some pickup ions collide and transfer energy and momentum to the neutral atmosphere of Titan, creating the visible asymmetry in the spatial distribution. The linear growth of pickup ion energy with distance indicates the presence of an average DC electric field around Titan. The source of this DC electric field is the convective electric field upstream of Titan. The estimate from the radial evolution of the PUI energy convective electric field is in relatively good agreement with that provided by CAPS IMS ion moments and magnetic field. This technique can be used outside the induced magnetosphere, where the convective electric field has the largest contribution compared with other terms in the generalized Ohm's law.

Our results are to some extent limited by instrumental capabilities, for example, the limited FOV of CAPS IMS does not allow for the resolution of pickup ions. Similarly, for the same reason, the TOF analysis is complicated due to the low count level and FOV limitations. A more refined analysis of pickup ions' pitch-angle distributions can be performed by transforming into the bulk plasma reference frame. For example, Radulescu et al. (2025) performed the analysis of the ion distribution function in Saturn's inner magnetosphere. As a part of the analysis, the authors calculate the pitch-angle distribution by subtracting the bulk plasma population from the distribution function. Using this method, the pickup ion's signature is more pronounced in the data. Similar approach has been shown to be valid at other planets and comets (e.g., Coates, 2017). However, in this paper, we use ion PADs for detection purposes, and the detailed analysis of the underlying physics goes beyond the scope of the study. The continuation of this study can be focused on the radial evolution of the ion distribution function and underlying physical processes. While collisional processes around Titan's induced magnetosphere can be largely neglected, the wave-particle interactions are yet to be discussed. As it was noted previously, wave activity around Titan has not been studied much, although it is likely to play a significant role. A better understanding of energization processes, in the absence of measurements, can be achieved with plasma simulations. Since we are interested in large-scale interactions with an emphasis on ion-scale physics, hybrid-Vlasov simulations would be beneficial.

5. Conclusions

In this work, magnetometer data from MAG, particle data from CAPS, and wave observations from RPWS were combined to present a global structure of Titan's induced magnetosphere and its ion pickup population. Data from the CAPS ELS electron spectrometer, together with plasma wave observations from RPWS, have provided, for the set of flybys from the TA to T82 flybys, a continuous electron density profile ranging from 10^{-2} to several 10^3 cm^{-3}. These profiles have been used to infer a global electron density map of Titan's near environment. The cold ionospheric plasma is confined on the ramside below $\approx$1.88 R_T to $\approx$2.15 R_T, while it has been observed to extend farther than 6 Titan radii in the wake region. The extended tail of electrons reaches at least 6 R_T, following the draped magnetic field lines in the magnetotail. It can be used to determine an upper limit of a cross-section tail area, required to compute total plasma loss rates, and to determine the average location of the induced magnetosphere in simulations. In the upstream of the induced magnetosphere, pickup ions have been observed and characterized with the IMS CAPS. The spatial distribution of pickup ions has been observed to be majorly populated on the +**E**-hemisphere, close to the magnetic equator, supporting theoretical or modeling results. A

progressive energization is also observed, and pickup ions with few keV have been identified as close as ≈2 Titan radii. From their energy signatures, the background convective electric field intensity is retrieved and compared to the convective electric field E_{conv}, calculated from plasma moments, and measured magnetic field E_{PUI}. The value of E_{PUI} varies between 0.05 mV m^{-1} and 1.92 mV m^{-1} and is in a good agreement for the electric field values ≤1 mV m^{-1}. For larger values of the convective electric field, the deviations are more significant. The reported results shed light on how pickup ions are energized in the induced magnetosphere of Titan and how it connects to the global structure of Titan's plasma environment.

Conflict of Interest

The authors declare no conflicts of interest relevant to this study.

Availability Statement

The RPWS-CASSINI Low Rate MFR/HFR data (data set ID CO-V/E/J/S/SS-RPWS-3-RDR-LRFULL-V1.0) used in this paper are available at the NASA Planetary Data System (https://pds-ppi.igpp.ucla.edu/search/view/?f=yes&id=pds://PPI/CO-V_E_J_S_SS-RPWS-3-RDR-LRFULL-V1.0). The authors are grateful to the French "Centre de Données sur la Physique des Plasmas" for access to the visualization tools AMDA. The data set ID used is *CO-V/E/J/S/SS-RPWS-3-RDR-LRFULL-V1.0* and data are available in the NASA Planetary Data System (Kurth et al., 2018).

Acknowledgments
KK and NE acknowledge funding from the Swedish Research Council (Vetenskapsrådet) under contract 2020-03962. NR is supported by NASA under award number 80GSFC24M0006. MKGH acknowledges financial support from the Taighde Éireann—Research Ireland under Grant number [22/PATH-S/10757]. AJC acknowledges partial support from STFC Grant ST/W001004/1, and the CAPS instrument and operations were supported by grants from STFC/PPARC (UK) and NASA JPL (USA). The authors are also grateful to SNSA (formerly SNSB) which supported the RPWS/LP instrument onboard Cassini. RM, JJB, PC, RP and FL are indebted to the "Soleil, Heliosphere, Magnetosphere" group of CNES for its support. It is based on observations with RPWS, CAPS, MAG embarked on Cassini.

References

Ågren, K., Wahlund, J., Garnier, P., Modolo, R., Cui, J., Galand, M., & Müller-Wodarg, I. (2009). On the ionospheric structure of Titan. *Planetary and Space Science*, *57*(14–15), 1821–1827. https://doi.org/10.1016/j.pss.2009.04.012

Arridge, C. S., Achilleos, N., & Guio, P. (2011). Electric field variability and classifications of Titan's magnetoplasma environment. *Annales Geophysicae*, *29*(7), 1253–1258. https://doi.org/10.5194/angeo-29-1253-2011

Arridge, C. S., André, N., Bertucci, C. L., Garnier, P., Jackman, C. M., Németh, Z., et al. (2011). Upstream of Saturn and Titan. *Space Science Reviews*, *162*(1–4), 25–83. https://doi.org/10.1007/s11214-011-9849-x

Arridge, C. S., André, N., McAndrews, H. J., Bunce, E. J., Burger, M. H., Hansen, K. C., et al. (2011). Mapping magnetospheric equatorial regions at Saturn from Cassini prime mission observations. *Space Science Reviews*, *164*(1–4), 1–83. https://doi.org/10.1007/s11214-011-9850-4

Arridge, C. S., Gilbert, L. K., Lewis, G. R., Sittler, E. C., Jones, G. H., Kataria, D. O., et al. (2009). The effect of spacecraft radiation sources on electron moments from the Cassini caps electron spectrometer. *Planetary and Space Science*, *57*(7), 854–869. https://doi.org/10.1016/j.pss.2009.02.011

Arridge, C. S., Russell, C. T., Khurana, K. K., Achilleos, N., Cowley, S. W. H., Dougherty, M. K., et al. (2008). Saturn's magnetodisc current sheet. *Journal of Geophysical Research*, *113*(A4), A04214. https://doi.org/10.1029/2007JA012540

Backes, H., Neubauer, F. M., Dougherty, M. K., Achilleos, N., André, N., Arridge, C. S., et al. (2005). Titan's magnetic field signature during the First Cassini Encounter. *Science*, *308*(5724), 992–995. https://doi.org/10.1126/science.1109763

Barabash, S. (2012). Classes of the solar wind interactions in the solar system. *Earth Planets and Space*, *64*(2), 57–59. https://doi.org/10.5047/eps.2012.01.005

Bertucci, C., Achilleos, N., Dougherty, M. K., Modolo, R., Coates, A. J., Szego, K., et al. (2008). The magnetic memory of Titan's ionized atmosphere. *Science*, *321*(5895), 1475–1478. https://doi.org/10.1126/science.1159780

Bertucci, C., Duru, F., Edberg, N., Fraenz, M., Martinecz, C., Szego, K., & Vaisberg, O. (2011). The induced magnetospheres of Mars, Venus, and Titan. *Space Science Reviews*, *162*(1–4), 113–171. https://doi.org/10.1007/s11214-011-9845-1

Bertucci, C., Sinclair, B., Achilleos, N., Hunt, P., Dougherty, M. K., & Arridge, C. S. (2009). The variability of Titan's magnetic environment. *Planetary and Space Science*, *57*(14–15), 1813–1820. https://doi.org/10.1016/j.pss.2009.02.009

Chatain, A., Wahlund, J. E., Shebanits, O., Hadid, L. Z., Morooka, M., Edberg, N. J. T., et al. (2021). Re-analysis of the Cassini RPWS/LP data in Titan's ionosphere: 1. Detection of several electron populations. *Journal of Geophysical Research: Space Physics*, *126*(8), e28412. https://doi.org/10.1029/2020JA028412

Chen, C., & Simon, S. (2020). A comprehensive study of Titan's magnetic pile-up region during the Cassini era. *Planetary and Space Science*, *191*, 105037. https://doi.org/10.1016/j.pss.2020.105037

Coates, A. J. (2009). Interaction of Titan's ionosphere with Saturn's magnetosphere. *Royal Society of London Philosophical Transactions Series A*, *367*(1889), 773–788. https://doi.org/10.1098/rsta.2008.0248

Coates, A. J. (2017). Pickup particle acceleration at Comets, Moons and magnetospheres. *Journal of Physics: Conference Series*, *900*, 012002. https://doi.org/10.1088/1742-6596/900/1/012002

Coates, A. J., Crary, F. J., Young, D. T., Szego, K., Arridge, C. S., Bebesi, Z., et al. (2007). Ionospheric electrons in Titan's tail: Plasma structure during the Cassini T9 encounter. *Geophysical Research Letters*, *34*(24). https://doi.org/10.1029/2007GL030919

Coates, A. J., Wellbrock, A., Lewis, G. R., Arridge, C. S., Crary, F. J., Young, D. T., et al. (2012). Cassini in Titan's tail: Caps observations of plasma escape. *Journal of Geophysical Research*, *117*(A5). https://doi.org/10.1029/2012JA017595

Cowee, M. M., Gary, S. P., Wei, H. Y., Tokar, R. L., & Russell, C. T. (2010). An explanation for the lack of ion cyclotron wave generation by pickup ions at Titan: 1-d hybrid simulation results. *Journal of Geophysical Research*, *115*(A10). https://doi.org/10.1029/2010JA015769

T. E. Cravens (1997). *Physics of solar system plasmas*.

Cravens, T. E., Yelle, R. V., Wahlund, J.-E., Shemansky, D. E., & Nagy, A. F. (2010). Composition and structure of the ionosphere and thermosphere. In R. H. Brown, J.-P. Lebreton, & J. H. Waite (Eds.), *Titan from Cassini-Huygens* (p. 259). https://doi.org/10.1007/978-1-4020-9215-2-11

21699402, 2026, 4, Downloaded from https://agupubs.onlinelibrary.wiley.com/doi/10.1029/2025JA034830 by Uppsala Universitet, Wiley Online Library on [08/05/2026]. See the Terms and Conditions (https://onlinelibrary.wiley.com/terms-and-conditions) on Wiley Online Library for rules of use; OA articles are governed by the applicable Creative Commons License

Dougherty, M., Kellock, S., Slootweg, A., Achilleos, N., Joy, S., & Mafi, J. (2023). Cassini MAG Calibrated 1 Sec. Avg. Data in KSO Coords. Collection. https://doi.org/10.17189/3N1M-4727

Dougherty, M. K., Kellock, S., Southwood, D. J., Balogh, A., Smith, E. J., Tsurutani, B. T., et al. (2004). The Cassini magnetic field investigation. *Space Science Reviews*, *114*(1–4), 331–383. https://doi.org/10.1007/s11214-004-1432-2

Dubinin, E., Modolo, R., Fraenz, M., Päetzold, M., Woch, J., Chai, L., et al. (2019). The induced magnetosphere of Mars: Asymmetrical topology of the magnetic field lines. *Geophysical Research Letters*, *46*(22), 12722–12730. https://doi.org/10.1029/2019GL084387

Edberg, N., Ågren, K., Wahlund, J.-E., Morooka, M., Andrews, D., Cowley, S., et al. (2011). Structured ionospheric outflow during the Cassini T55–T59 Titan flybys. *Planetary and Space Science*, *59*(8), 788–797. https://doi.org/10.1016/j.pss.2011.03.007

Edberg, N. J. T., Andrews, D. J., Bertucci, C., Gurnett, D. A., Holmberg, M. K. G., Jackman, C. M., et al. (2015). Effects of Saturn's magnetospheric dynamics on Titan's ionosphere. *Journal of Geophysical Research: Space Physics*, *120*(10), 8884–8898. https://doi.org/10.1002/2015JA021373

Edberg, N. J. T., Andrews, D. J., Shebanits, O., Ågren, K., Wahlund, J., Opgenoorth, H. J., et al. (2013). Solar cycle modulation of Titan's ionosphere. *Journal of Geophysical Research: Space Physics*, *118*(8), 5255–5264. https://doi.org/10.1002/jgra.50463

Edberg, N. J. T., Wahlund, J.-E., Ågren, K., Morooka, M. W., Modolo, R., Bertucci, C., & Dougherty, M. K. (2010). Electron density and temperature measurements in the cold plasma environment of Titan: Implications for atmospheric escape. *Geophysical Research Letters*, *37*(20), 20105. https://doi.org/10.1029/2010GL044544

Felici, M., Arridge, C. S., Wilson, R. J., Coates, A. J., Thomsen, M., & Reisenfeld, D. (2018). Survey of thermal plasma composition in Saturn's magnetosphere using time-of-flight data from Cassini/Caps. *Journal of Geophysical Research: Space Physics*, *123*(8), 6494–6513. https://doi.org/10.1029/2017JA025085

Garnier, P., Dandouras, I., Toublanc, D., Roelof, E. C., Brandt, P. C., Mitchell, D. G., et al. (2010). Statistical analysis of the energetic ion and ENA data for the Titan environment. *Planetary and Space Science*, *58*(14–15), 1811–1822. https://doi.org/10.1016/j.pss.2010.08.009

Gurnett, D. A., Kurth, W. S., Kirchner, D. L., Hospodarsky, G. B., Averkamp, T. F., Zarka, P., et al. (2004). The Cassini radio and plasma wave investigation. *Space Science Reviews*, *114*(1–4), 395–463. https://doi.org/10.1007/s11214-004-1434-0

Gustafsson, G., & Wahlund, J. E. (2010). Electron temperatures in Saturn's plasma disc. *Planetary and Space Science*, *58*(7–8), 1018–1025. https://doi.org/10.1016/j.pss.2010.03.007

Halekas, J. S., Brain, D. A., Luhmann, J. G., DiBraccio, G. A., Ruhunusiri, S., Harada, Y., et al. (2017). Flows, fields, and forces in the mars-solar wind interaction. *Journal of Geophysical Research: Space Physics*, *122*(11), 11320–11341. https://doi.org/10.1002/2017JA024772

Hartle, R. E., Sarantos, M., & Sittler, E. C., Jr. (2011). Pickup ion distributions from three-dimensional neutral exospheres. *Journal of Geophysical Research*, *116*(A15), 10101. https://doi.org/10.1029/2011JA016859

Hartle, R. E., & Sittler, E. C. (2007). Pickup ion phase space distributions: Effects of atmospheric spatial gradients. *Journal of Geophysical Research*, *112*(A7), 7104. https://doi.org/10.1029/2006JA012157

Hartle, R. E., Sittler, E. C., Neubauer, F. M., Johnson, R. E., Smith, H. T., Crary, F., et al. (2006). Preliminary interpretation of Titan plasma interaction as observed by the Cassini Plasma Spectrometer: Comparisons with Voyager 1. *Geophysical Research Letters*, *33*(8), 8201. https://doi.org/10.1029/2005GL024817

Hartle, R. E., Sittler, E. C., Ogilvie, K. W., Scudder, J. D., Lazarus, A. J., & Atreya, S. K. (1982). Titan's ion exosphere observed from Voyager 1. *Journal of Geophysical Research*, *87*(A3), 1383–1394. https://doi.org/10.1029/JA087iA03p01383

Holmberg, M. K. G., Wahlund, J. E., & Morooka, M. W. (2014). Dayside/nightside asymmetry of ion densities and velocities in Saturn's inner magnetosphere. *Geophysical Research Letters*, *41*(11), 3717–3723. https://doi.org/10.1002/2014GL060229

Kabanovic, S., Simon, S., Neubauer, F. M., & Meeks, Z. (2017). An empirical model of Titan's magnetic environment during the Cassini era: Evidence for seasonal variability. *Journal of Geophysical Research: Space Physics*, *122*(11), 11076–11085. https://doi.org/10.1002/2017JA024402

Kim, K., Edberg, N. J. T., Wahlund, J.-E., & Vigren, E. (2024). Alfvén wing-like structures in Titan's magnetotail during T122-T126 flybys. *Journal of Geophysical Research: Space Physics*, *129*(6), e2023JA032265. https://doi.org/10.1029/2023JA032265

Kurth, W., Johnson, R., & G, L. J. (2018). *Cassini V/E/J/S/SS RPWS calibrated low rate full res v1.0, co-v/e/j/s/ss-rpws-3-rdr-lrfull-v1.0*. NASA Planetary Data System. Retrieved from https://pds-ppi.igpp.ucla.edu/collection/urn:nasa:pds:cassini-caps-derived:data-ele-mom

Ledvina, S. A., Brecht, S. H., & Cravens, T. E. (2012). The orientation of Titan's dayside ionosphere and its effects on Titan's plasma interaction. *Earth Planets and Space*, *64*(2), 207–230. https://doi.org/10.5047/eps.2011.08.009

Lewis, G. R., André, N., Arridge, C. S., Coates, A. J., Gilbert, L. K., Linder, D. R., & Rymer, A. M. (2008). Derivation of density and temperature from the Cassini Huygens CAPS electron spectrometer. *Planetary and Space Science*, *56*(7), 901–912. https://doi.org/10.1016/j.pss.2007.12.017

Luhmann, J. G. (1996). Titan's ion exosphere wake: A natural ion mass spectrometer? *Journal of Geophysical Research*, *101*(E12), 29387–29393. https://doi.org/10.1029/96JE03307

Ma, Y., Nagy, A. F., Cravens, T. E., Sokolov, I. V., Hansen, K. C., Wahlund, J.-E., et al. (2006). Comparisons between MHD model calculations and observations of Cassini flybys of Titan. *Journal of Geophysical Research*, *111*(A5), 5207. https://doi.org/10.1029/2005JA011481

Modolo, R., & Chanteur, G. M. (2008). A global hybrid model for Titan's interaction with the Kronian plasma: Application to the Cassini Ta flyby. *Journal of Geophysical Research*, *113*(A12), 1317. https://doi.org/10.1029/2007JA012453

Modolo, R., Chanteur, G. M., Wahlund, J.-E., Canu, P., Kurth, W. S., Gurnett, D., et al. (2007). Plasma environment in the wake of Titan from hybrid simulation: A case study. *Geophysical Research Letters*, *34*(24). https://doi.org/10.1029/2007GL030489

Modolo, R., Wahlund, J., Boström, R., Canu, P., Kurth, W. S., Gurnett, D., et al. (2007). Far plasma wake of Titan from the RPWS observations: A case study. *Geophysical Research Letters*, *34*, 24. https://doi.org/10.1029/2007GL030482

Morooka, M., Modolo, R., Wahlund, J. E., André, M., Eriksson, A. I., Persoon, D. A., et al. (2009). The electron density of Saturn's magnetosphere. *Annales Geophysicae*, *27*(7), 2971–2991. https://doi.org/10.5194/angeo-27-2971-2009

Morooka, M. W., Wahlund, J. E., Eriksson, A. I., Farrell, W. M., Gurnett, D. A., Kurth, W. S., et al. (2011). Dusty plasma in the vicinity of Enceladus. *Journal of Geophysical Research*, *116*(A12), A12221. https://doi.org/10.1029/2011JA017038

Nelson, D., & Berthelier, J. J. (2009). *Caps simulator, handbook* (Tech. Rep.). LATMOS.

Németh, Z., Szego, K., Bebesi, Z., Erdős, G., Foldy, L., Rymer, A., et al. (2011). Ion distributions of different Kronian plasma regions. *Journal of Geophysical Research*, *116*(A9), A09212. https://doi.org/10.1029/2011JA016585

Neubauer, F. M., Backes, H., Dougherty, M. K., Wennmacher, A., Russell, C. T., Coates, A., et al. (2006). Titan's near magnetotail from magnetic field and electron plasma observations and modeling: Cassini flybys TA, TB, and T3. *Journal of Geophysical Research*, *111*(A10), 10220. https://doi.org/10.1029/2006JA011676

Radulescu, C. R., Coates, A. J., Simon, S., Verscharen, D., & Jones, G. H. (2025). Pick-up ion distributions in the inner and middle Saturnian magnetosphere. *Journal of Geophysical Research: Space Physics*, *130*(1), 2024JA033390. https://doi.org/10.1029/2024JA033390

21699402, 2026, 4, Downloaded from https://agupubs.onlinelibrary.wiley.com/doi/10.1029/2025JA034830 by Uppsala Universitet, Wiley Online Library on [08/05/2026]. See the Terms and Conditions (https://onlinelibrary.wiley.com/terms-and-conditions) on Wiley Online Library for rules of use; OA articles are governed by the applicable Creative Commons License

Regoli, L. H., Coates, A. J., Thomsen, M. F., Jones, G. H., Roussos, E., Waite, J. H., et al. (2016). Survey of pickup ion signatures in the vicinity of Titan using CAPS/IMS. *Journal of Geophysical Research: Space Physics*, *121*(9), 8317–8328. https://doi.org/10.1002/2016JA022617

Regoli, L. H., Roussos, E., Dialynas, K., Luhmann, J. G., Sergis, N., Jia, X., et al. (2018). Statistical study of the energetic proton environment at Titan's orbit from the Cassini spacecraft. *Journal of Geophysical Research: Space Physics*, *123*(6), 4820–4834. https://doi.org/10.1029/2018JA025442

Romanelli, N., Modolo, R., Dubinin, E., Berthelier, J.-J., Bertucci, C., Wahlund, J. E., et al. (2014). Outflow and plasma acceleration in Titan's induced magnetotail: Evidence of magnetic tension forces. *Journal of Geophysical Research: Space Physics*, *119*(12), 9992–10005. https://doi.org/10.1002/2014JA020391

Rymer, A. M., Smith, H. T., Wellbrock, A., Coates, A. J., & Young, D. T. (2009). Discrete classification and electron energy spectra of Titan's varied magnetospheric environment. *Geophysical Research Letters*, *36*(15), 15109. https://doi.org/10.1029/2009GL039427

Shebanits, O., Vigren, E., Wahlund, J. E., Holmberg, M. K. G., Morooka, M., Edberg, N. J. T., et al. (2017). Titan's ionosphere: A survey of solar EUV influences. *Journal of Geophysical Research: Space Physics*, *122*(7), 7491–7503. https://doi.org/10.1002/2017JA023987

Shebanits, O., Wahlund, J. E., Edberg, N. J. T., Crary, F. J., Wellbrock, A., Andrews, D. J., et al. (2016). Ion and aerosol precursor densities in Titan's ionosphere: A multi-instrument case study. *Journal of Geophysical Research: Space Physics*, *121*(10). https://doi.org/10.1002/2016JA022980

Sillanpää, I., Kallio, E., Janhunen, P., Schmidt, W., Mursula, K., Vilppola, J., & Tanskanen, P. (2006). Hybrid simulation study of ion escape at Titan for different orbital positions. *Advances in Space Research*, *38*(4), 799–805. https://doi.org/10.1016/j.asr.2006.01.005

Simon, S., Boesswetter, A., Bagdonat, T., Motschmann, U., & Schuele, J. (2007). Three-dimensional multispecies hybrid simulation of Titan's highly variable plasma environment. *Annales Geophysicae*, *25*(1), 117–144. https://doi.org/10.5194/angeo-25-117-2007

Simon, S., Neubauer, F. M., Wennmacher, A., & Dougherty, M. K. (2014). Variability of Titan's induced magnetotail: Cassini magnetometer observations. *Journal of Geophysical Research: Space Physics*, *119*(3), 2024–2037. https://doi.org/10.1002/2013JA019608

Simon, S., van Treeck, S. C., Wennmacher, A., Saur, J., Neubauer, F. M., Bertucci, C. L., & Dougherty, M. K. (2013). Structure of Titan's induced magnetosphere under varying background magnetic field conditions: Survey of Cassini magnetometer data from flybys TA–T85. *Journal of Geophysical Research: Space Physics*, *118*(4), 1679–1699. https://doi.org/10.1002/jgra.50096

Simon, S., Wennmacher, A. M. N., Bertucci, C. L., Kriegel, H., Saur, J., Russell, C. T., et al. (2010). Titan's highly dynamicmagnetic environment: A systematic survey of Cassini magnetometer observations from flybys TA-T62. *Planetary and Space Science*. https://doi.org/10.1016/j.pss.2010.04.021

Sittler, E. C., Hartle, R. E., Johnson, R. E., Cooper, J. F., Lipatov, A. S., Bertucci, C., et al. (2010). Saturn's magnetospheric interaction with Titan as defined by Cassini encounters T9 and T18: New results. *Planetary and Space Science*, *58*(3), 327–350. https://doi.org/10.1016/j.pss.2009.09.017

Smith, H., Crary, F., Reisenfeld, D., Shappirio, M., Sittler, E., & Woodson, A. (2019). Caps IMS time-of-flight analysis TOF procedures.

Smith, H. T., & Rymer, A. M. (2014). An empirical model for the plasma environment along Titan's orbit based on Cassini plasma observations. *Journal of Geophysical Research: Space Physics*, *119*(7), 5674–5684. https://doi.org/10.1002/2014JA019872

Snowden, D., Winglee, R., Bertucci, C., & Dougherty, M. (2007). Three-dimensional multifluid simulation of the plasma interaction at Titan. *Journal of Geophysical Research*, *112*(A11), 12221. https://doi.org/10.1029/2007JA012393

Szego, K., Bebesi, Z., Bertucci, C., Coates, A. J., Crary, F., Erdos, G., et al. (2007). Charged particle environment of Titan during the T9 flyby. *Geophysical Research Letters*, *34*, 24. https://doi.org/10.1029/2007GL030677

Szegö, K., Glassmeier, K.-H., Bingham, R., Bogdanov, A., Fischer, C., Haerendel, G., et al. (2000). Physics of mass loaded plasmas. *Space Science Reviews*, *94*(3–4), 429–671. https://doi.org/10.1023/A:1026568530975

Thomsen, M. F., Reisenfeld, D. B., Delapp, D. M., Tokar, R. L., Young, D. T., Crary, F. J., et al. (2010). Survey of ion plasma parameters in Saturn's magnetosphere. *Journal of Geophysical Research*, *115*(A10). https://doi.org/10.1029/2010JA015267

Thomsen, M. F., Reisenfeld, D. B., Wilson, R. J., Andriopoulou, M., Crary, F. J., Hospodarsky, G. B., et al. (2014). Ion composition in interchange injection events in Saturn's magnetosphere. *Journal of Geophysical Research: Space Physics*, *119*(12), 9761–9772. https://doi.org/10.1002/2014JA020489

Vigren, E., Galand, M., Yelle, R. V., Cui, J., Wahlund, J. E., Ågren, K., et al. (2013). On the thermal electron balance in Titan's sunlit upper atmosphere. *Icarus*, *223*(1), 234–251. https://doi.org/10.1016/j.icarus.2012.12.010

Vigren, E., Galand, M., Yelle, R. V., Wellbrock, A., Coates, A. J., Snowden, D., et al. (2015). Ionization balance in Titan's nightside ionosphere. *Icarus*, *248*, 539–546. https://doi.org/10.1016/j.icarus.2014.11.012

Wahlund, J.-E., Boström, R., Gustafsson, G., Gurnett, D. A., Kurth, W. S., Pedersen, A., et al. (2005). Cassini measurements of cold plasma in the ionosphere of Titan. *Science*, *308*(5724), 986–989. https://doi.org/10.1126/science.1109807

Wahlund, J.-E., Modolo, R., Bertucci, C., & Coates, A. (2014). Titan's magnetospheric and plasma environment. In I. Müller-Wodarg, C. A. Griffith, E. Lellouch, & T. E. Cravens (Eds.), *Titan: Surface, atmosphere and magnetosphere*. Cambridge University Press.

Waite, J. H. (2022). Cassini-Huygens plasma spectrometer (CAPS) derived electron moments data collection. *NASA Planetary Data System, urn:nasa:pds:cassini-caps-derived:data-ele-mom::1.0*. https://doi.org/10.17189/NZK5-RQ31

Waite, J. H., & Furman, J. D. (2022). Cassini-Huygens Cassini plasma spectrometer (CAPS) derived ion moments data collection. *NASA Planetary Data System, urn:nasa:pds:cassini-caps-derived:data-ion-moments::1.0*. https://doi.org/10.17189/0TG3-2Z14

Waite, J. H., Lewis, W. S., Kasprzak, W. T., Anicich, V. G., Block, B. P., Cravens, T. E., et al. (2004). The Cassini ion and neutral mass spectrometer (INMS) investigation. *Space Science Reviews*, *114*(1–4), 113–231. https://doi.org/10.1007/s11214-004-1408-2

Wei, H. Y., Russell, C. T., Dougherty, M. K., Neubauer, F. M., & Ma, Y. J. (2010). Upper limits on Titan's magnetic moment and implications for its interior. *Journal of Geophysical Research*, *115*(E10), E10007. https://doi.org/10.1029/2009JE003538

Westlake, J. H., Paranicas, C. P., Cravens, T. E., Luhmann, J. G., Mandt, K. E., Smith, H. T., et al. (2012). The observed composition of ions outflowing from Titan. *Geophysical Research Letters*, *39*(19). https://doi.org/10.1029/2012GL053079

Wilson, R. J. (2021). Cassini CAPS fitted parameters bundle. *NASA Planetary Data System, urn:nasa:pds:cassini-caps-fitted-parameters::1.0*. https://doi.org/10.17189/1521149

Wilson, R. J., Bagenal, F., & Persoon, A. M. (2017). Survey of thermal plasma ions in Saturn's magnetosphere utilizing a forward model. *Journal of Geophysical Research: Space Physics*, *122*(7), 7256–7278. https://doi.org/10.1002/2017JA024117

Wilson, R. J., Crary, F., Gilbert, L. K., Reisenfeld, D. B., Steinberg, J. T., & Livi, R. (2012). *PDS user's guide for Cassini plasma spectrometer*. PDS. Retrieved from https://pds-ppi.igpp.ucla.edu/

Young, D. T., Berthelier, J. J., Blanc, M., Burch, J. L., Coates, A. J., Goldstein, R., et al. (2004). Cassini plasma spectrometer investigation. *Space Science Reviews*, *114*(1–4), 1–112. https://doi.org/10.1007/s11214-004-1406-4

21699402, 2026, 4, Downloaded from https://agupubs.onlinelibrary.wiley.com/doi/10.1029/2025JA034830 by Uppsala Universitet, Wiley Online Library on [08/05/2026]. See the Terms and Conditions (https://onlinelibrary.wiley.com/terms-and-conditions) on Wiley Online Library for rules of use; OA articles are governed by the applicable Creative Commons License